

# Influence of the Molecular Structure on Slow Crack Growth Resistance and Impact Fracture Toughness in Cr-Catalyzed Ethylene–Hexene Copolymers for Pipe Applications

V. STEPHENNE,<sup>1</sup> D. DAOUST,<sup>1</sup> G. DEBRAS,<sup>2</sup> M. DUPIRE,<sup>2</sup> R. LEGRAS,<sup>1</sup> J. MICHEL<sup>2</sup>

<sup>1</sup> Unité de Physique et de Chimie des Hauts Polymères, Université Catholique de Louvain, 1, Place Croix du Sud, B-1348 Louvain-la-Neuve, Belgium

<sup>2</sup> Fina Research S.A., Zone industrielle C, B-7181 Feluy-Seneffe, Belgium

Received 25 February 2000; accepted 18 November 2000

**ABSTRACT:** In this study we correlate parameters describing molecular structure (molar mass distribution, short chain branching content, intermolecular heterogeneity) of different ethylene–hexene Cr-catalyzed copolymers, with slow crack growth and rapid crack propagation resistances, respectively measured with Bent Strip and Charpy tests. The PTREF technique, coupled with classical techniques, was used. Two new indices were proposed to correlate mechanical properties and molecular structure. © 2001 John Wiley & Sons, Inc. *J Appl Polym Sci* 82: 916–928, 2001

**Key words:** polyethylene; pipes; slow crack growth; rapid crack propagation; molecular structure; TREF

## INTRODUCTION

A durable service lifetime for polyethylene (PE) pipes under pressure requires an excellent resistance to slow crack growth (SCG) and to environmental stress cracking (ESC). Another potential failure is rapid crack propagation (RCP), occurring after external impact. Factors affecting these different mechanisms of failure have been extensively discussed previously in literature. SCG is a brittle failure, appearing for low stress and after relatively long times.<sup>1,2</sup> Two processes control the rate of SCG: the initiation rate of the craze as it precedes the crack and the rate of crack propagation. The latter process is the controlling mecha-

nism in  $\alpha$ -olefin/ethylene copolymers and is governed by the disentanglement rate of tie molecules into fibrils, at the base of the craze.<sup>3</sup> The lower the disentanglement rate, the higher the resistance to SCG. Although this rate mainly depends on the content of tie molecules, it also depends on their spatial configuration, their entanglement efficiency, and the strength of the crystals in which they are anchored.

Different molecular and morphological parameters influencing slow crack growth resistance (SCGR), after extrusion of the pipe, are given in the literature: the molar mass, the molar mass distribution, the type of short chain branching (SCB), the SCB content, the repartition of the SCB on the macromolecules (intra- and intermolecular heterogeneities), the lamellar thicknesses distribution, and both the density (crystallinity) and the lamellar orientation of the sample.<sup>3–8</sup> The presence of longer molecules leads to im-

Correspondence to: V. Stephenne (stephenne@poly.ucl.ac.be).  
Contract grant sponsor: La Région Wallonne.

*Journal of Applied Polymer Science*, Vol. 82, 916–928 (2001)  
© 2001 John Wiley & Sons, Inc.

proved SCGR because of more tie molecules,<sup>9</sup> more effective tie molecule entanglements,<sup>10</sup> and anchoring in the crystalline lamellae.<sup>3</sup> Several authors indicate, however, that no tie molecules could be observed below a critical molar mass. This value is not unique for PE but depends on the SCB content. SCGR increases with broader molar mass distribution.<sup>11</sup> Incorporation of comonomer increases the content of tie molecules and the efficiency of the entanglements. Branching also decreases the lamellar thickness, thus its strength and the tie chains' anchoring.<sup>5,12</sup> Thus the optimum SCGR is reached with an intermediate comonomer content. Bubeck and Baker<sup>13</sup> found that increasing the branch length from methyl to hexyl increases SCGR as a result of more effective tie chain entanglements. Several authors<sup>11,14,15</sup> showed that a better SCGR is obtained with the highest comonomer concentration on the longest molecules. This can be attributed to a stronger entanglement in the longest macromolecules because the longer the molecule, the greater the likelihood of its being a tie molecule.

SCG can be accelerated in the presence of an aggressive environment like Igepal.<sup>16</sup> The resistance to this type of failure is called environmental stress cracking resistance (ESC). It occurs at a stress level largely inferior to the one required in air.<sup>17</sup>

More seldom but more insidious than SCG, RCP is a brittle failure, occurring after sufficient impact.<sup>18</sup> No mechanism leading to its occurrence has been clearly identified up to now. Nevertheless, experimental results are reported in the literature. In general, impact fracture toughness increases when the molecules are longer.<sup>19–21</sup> A narrow molar mass distribution is also favorable.<sup>19</sup> Several authors indicate a decrease of the resistance to impact with increasing density.<sup>22,23</sup> However, such a trend has not been distinctly observed by Fleissner,<sup>19</sup> who noticed that the impact toughness becomes nearly independent of density above a critical density value.

“PE63” is the brand name of the first generation of PEs for pipe applications, introduced at the end of the 1950s. These high-density polyethylenes (HDPE, i.e., PE with a density above 0.940) are homopolymers, characterized by a good resistance to creep.

The second generation of PEs, called “PE80,” were characterized by a better SCGR than the previous PE63 because of incorporation of comonomers. However, these medium-density polyethylenes (MDPE, i.e., with a density be-

tween 0.926 and 0.940) have a lower creep resistance. It must also be emphasized that intermolecular heterogeneity of these copolymers, obtained with Ziegler–Natta or chromium catalyst, does not seem optimum in terms of SCGR. Indeed, several authors, mainly for Ziegler–Natta-catalyzed PE materials,<sup>24–27</sup> show that SCB are mainly situated on shorter molecules.

The last evolution (third generation called “PE100”) consists of mixing low molar mass homopolymer molecules with larger molar mass copolymer molecules. Thus, SCB are mainly situated on longer macromolecules, resulting in a better SCGR while the high density low molar mass fraction confers a resistance to creep comparable to that of “PE63.”

In this study we try to correlate some parameters describing molecular structure (average molar masses, molar mass distribution, SCB content, intermolecular heterogeneity) with rapid and slow crack propagations in ethylene–hexene copolymers. For this purpose, new indices are proposed in this study. These copolymers (two MDPEs and three HDPEs) were synthesized with Cr-catalysts in different conditions of polymerization, to modify the repartition of the comonomer on the different macromolecules of these products.

The main consideration is the influence of the molecular structure on mechanical properties. Possible morphological effects are not really taken into account in this work. For example, lamellar thickness measurements are not attempted. Only melting and crystallization temperatures, crystallinities [both by differential scanning calorimetry (DSC)], and density measurements (by pycnometer) are carried out.

The mechanical properties are evaluated with laboratory scale tests (environmental Bent Strip Test for SCG and Charpy Test for RCP) on compression-molded samples. Molecular structure is studied by means of two different approaches. The first, a classical approach, consists of analyzing the neat samples (pellets) with conventional characterization techniques [nuclear magnetic resonance (NMR), size-exclusion chromatography (SEC)]. In the second, original approach, the coupling of such classical techniques with fractionation techniques [stepwise isothermal segregation technique (SIST), preparative temperature rising elution fractionation (PTREF)] is presented, to study molecular structure more precisely. Intermolecular heterogeneity of Cr-catalyzed PE copolymers was confirmed by these techniques.

**Table I** Some Characteristics of the Five PE Samples Used in This Work

Reference	$T_m^a$	Density <sup>b</sup>	SCB Content <sup>c</sup>	$M_w^d$	$M_n^d$	$M_z^d$	$H^e$
Sample A	127.9	0.937	54	188,500	17,100	1,432,500	11.1
Sample B	127.4	0.933	68	205,500	14,800	1,460,200	14.1
Sample C	130.3	0.943	25	214,200	17,900	1,417,600	12.5
Sample D	132.3	0.945	20	230,300	22,300	1,519,500	10.5
Sample E	130.8	0.944	21	178,000	20,900	1,059,000	8.5

<sup>a</sup> Melting temperature determined by DSC (in °C) at 10°C/min.

<sup>b</sup> Density at 23°C in g/cm<sup>3</sup>.

<sup>c</sup> Butyl content measured by <sup>13</sup>C-NMR (/10,000 C).

<sup>d</sup> Weight-, number-, and *z*-average molar masses ( $M_n$ ,  $M_w$ ,  $M_z$ ) in daltons.

<sup>e</sup> Polydispersity index ( $H = M_w/M_n$ ).

## EXPERIMENTAL

### Materials

Five ethylene–hexene copolymers (A, B, C, D, and E), used in pipe applications, were studied. They are all monomodal PEs of the second generation (PE80). They were obtained by supported Cr-catalysts. Samples A and B were classified as medium-density polyethylenes (MDPE). Copolymers C, D, and E were high-density polyethylenes (HDPE). Density, melting temperatures, SCB content, and average molar mass values for these products are summarized in Table I. Pycnometer measurements confirm that samples A and B can be appropriately classified as MDPE, whereas other samples are HDPE. These latter contain significantly less SCB and present higher melting temperatures. Number-average and weight-average molar masses ( $M_n$  and  $M_w$ , respectively) of all copolymers, although not identical, lie in the same range. This comment, however, is not true when observing *z*-average molar masses ( $M_z$ ) obtained. Indeed, sample E, characterized by a significantly lower  $M_z$  value, contains far fewer long molecules. All five PEs are characterized by a large polydispersity index ( $H$ ), typical of multisite catalysts and ranging from 8.5 (sample E) to 14.1 (sample B).

### Mechanical Properties

#### Processing Step

Prior to mechanical testing, the PE pellets were compression-molded between Mylar films at 175°C into 3.2- or 1.95-mm-thick sheets (for Charpy Test or Bent Strip Test, respectively). For both sheets, the following compression-molding procedure was applied: 20 min at 175°C without pressure followed by 10 min under pressure (110

kN on 24 × 24-cm plaque, 1.9 MPa) at that temperature and a programmed constant cooling rate of 15°C/min (ASTM D-1928 procedure C).

### Charpy Test

Impact fracture toughness was evaluated, at a laboratory scale, with a Charpy instrumented impact tester Fractovis from CEAST. Interest in such a small-scale test (compared to industrial tests S4 and full-scale) to evaluate resistance to RCP was previously discussed in the literature.<sup>28,29</sup>

Single-edge notched bending (SENB) specimens were machined from the 3.2-mm-thick compression-molded sheets to their dimensions: length, 63.5 mm; width, 12.6 to 12.8 mm; notch depth, 6.35 mm; notch tip radius, 0.025 mm. The span-to-width ratio was fixed at 4 (span length 50.8 mm). Finally, the edge of a fresh razor blade was applied into the tip of the V-notched crack, resulting in a sharp crack of about 100 μm ahead of the machine crack tip.

The total energy absorbed by the SENB specimen was measured at the temperature of −10°C. The temperature of −10°C was chosen because at that temperature the grads were better discriminated (semi-ductile failure). Test parameters were: number of tests, 6; test time, 16 ms; hammer type, M 749; hammer weight, 5.154 kg; hammer speed, 1.07 m/s; impact height, 0.058 m; incident energy, 2.95 J; and support span, 50.8 mm.

### Bent Strip Test

SCGR is evaluated with an environmental test called Bent Strip Test (ASTM procedure D 1693), in which the SCG mechanism is accelerated by the presence of Igepal, an aggressive environment.<sup>16</sup> The test is run under the most severe

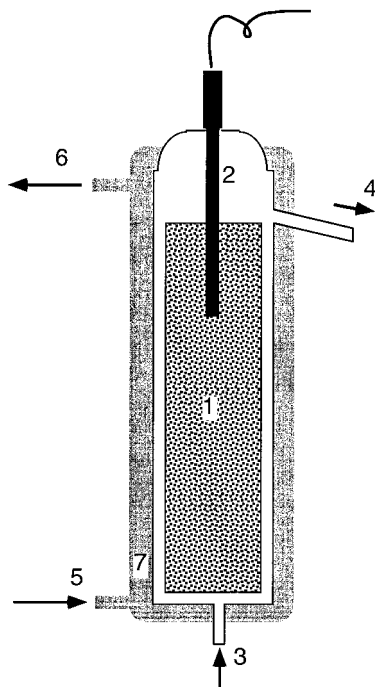


**Figure 1** PTREF column installation (1, inert support; 2, Pt100 probe; 3, solvent inlet; 4, solvent outlet; 5, oil bath inlet; 6, oil bath outlet; 7, oil jacket).

conditions, that is, in a 35 wt % Igepal solution at a temperature of 70°C. Elapsed time after statistical appearance of cracks in half of the 10 specimens tested is called  $F_{50}$ . This time is obtained by a graphical method described in the ASTM procedure.

#### **Preparative Temperature Rising Elution Fractionation (PTREF)**

Fractionation of the five resins, in terms of their crystallizability, was accomplished by a homemade apparatus preparative temperature rising elution fractionation (PTREF). The schematic of the apparatus used in this study was similar to the system of PTREF described by Wild and Ryle<sup>30</sup> and is presented in Figure 1. The insulated column was 600 mm high and 45 mm in diameter. It was filled with iron mesh as inert support. The temperature of the column was controlled using a Julabo F32 HP thermal controller (30–200 ± 0.05°C). The sample (≈6 g) was dissolved, under magnetic stirring, at 120°C in 400 mL of technical xylene, stabilized with Irganox 1010 antioxidant (2 g/L), and then loaded into the column preheated to 130°C. The system was kept isothermally at 130°C for a period of 60 min.

The PTREF technique can be divided into two sequential stages, precipitation and elution. In

the precipitation step, the column was cooled to a temperature of 30°C at the rate of 0.04°C/min. During the cooling of the diluted solution, the PE resin crystallizes onto the steel packing, forming thin layers with respect to their crystallizability, mainly determined by the longest average ethylene (crystallizable) sequence, starting from the support surface.

In the second step, the column was heated to 40°C (first elution temperature) at a rate of 1°C/min. The following stabilization temperature step lasted 20 min. Xylene, stabilized with Irganox 1010 (2 g/L) and preheated to the elution temperature, was passed upward through the column at a flow rate of 10 mL/min. The elution operation was stopped when no more precipitate was observed coming from the column into the methanol-filled vessel. The extraction temperature was raised in small intervals over the range 40–105°C. Eleven fractions, corresponding to successive elutions at temperatures of 40, 50, 60, 70, 80, 85, 90, 93, 96, 100, and 105°C, were thus obtained.

For all fractions, the polymer eluted was precipitated in a large excess of nonsolvent methanol, filtered, stabilized with Irganox 1010 (2000 ppm), dried at 50°C, and eventually weighed.

### **Characterization Techniques**

#### **Pycnometer**

Density was measured with a helium ACCUPYC 1330 pycnometer on the compression-molded SENB samples, according to an internal Fina Chemicals procedure. The value of the density is reported at a reference temperature of 23°C while the experiment is carried out at a temperature close to 29°C. For this, a density increase of  $3.6 \times 10^{-4}$  g/cm<sup>3</sup> per decrease of one degree was assumed. The measurement was accomplished on Charpy samples, after the test; the time after compression-molding was the same for all five resins (about 1 month).

#### **Size-Exclusion Chromatography (SEC)**

Molar mass and molar mass distribution were measured with an ALC/GPC 150C instrument (Waters Instruments, Rochester, MN), equipped with two AT-806 MS Shodex columns (Showa Denko, Japan) and one styragel 300-Å column (Waters Instruments). The solvent used was 1,2,4-trichlorobenzene, stabilized with Irganox 1010 (2 g/L). The polymer concentration in solution was 2 g/L. All measurements were carried

out at 135°C. Polystyrene standards were used for calibration purposes. By using the Mark–Houwink equations of polystyrene (PS) and PE, the molar masses, with respect to polystyrene, were converted to polyethylene. The Mark–Houwink constants ( $k$ ,  $\alpha$ ), generally used for HDPE, were also adopted for LLDPE, given that the hydrodynamic volume is not significantly affected by the presence of SCB in LLDPE. The values of the Mark–Houwink constants for PS and PE (in dL/g) were<sup>31,32</sup>

$$[\eta]_{\text{PS}} = 1.21 \cdot 10^{-4} \cdot M^{0.710}$$

$$[\eta]_{\text{PE}} = 5.10 \cdot 10^{-4} \cdot M^{0.706}$$

### Nuclear Magnetic Resonance Spectroscopy (NMR)

Butyl content was determined on unfractionated PE by <sup>13</sup>C–NMR spectroscopy. The spectra were recorded at 130°C on a Bruker 300-MHz NMR spectrometer (Bruker Instruments, Billerica, MA; Germany, Karlsruhe). Detailed parameters of the experiment were: pulse angle, 90°; delay time, 15 s; and acquisition time, 1.7 s.

Methyl content of PTREF fractions was obtained by <sup>1</sup>H–NMR spectroscopy, with a Bruker 300-MHz spectrometer at 130°C. Instrumental conditions were: pulse angle, 90°; delay time, 10 s; acquisition time, 2–4 s; and number of scans, 100–1000.

The polymer solutions were prepared by dissolving 5 mg polymer in 1 mL protonated/deuterated (70/30) paradichlorobenzene. Chemical shifts were referenced to an internal hexamethylene disiloxane (HMDS) standard and corrected to tetramethylsilane (TMS) by adding 2.03 ppm.

### Differential Scanning Calorimetry (DSC)

Thermal analysis was carried out using a differential scanning calorimeter Perkin–Elmer DSC7 (Perkin Elmer Cetus, Norwalk, CT). A weighed ( $\cong 10$  mg) sample was sealed in an aluminum pan and was subjected to a heating–cooling–heating cycle. Previous thermal effects were minimized by initially heating the samples until they melted. Subsequently, the cooling–heating cycle was recorded, providing exothermic (crystallization) and endothermic (melting) curves. The heating and cooling rates were 10°C/min and the range of temperatures examined was between –20°C and 220°C.

### Stepwise Isothermal Segregation Technique (SIST)

SIST<sup>33</sup> was carried out using a differential scanning calorimeter Perkin–Elmer DSC7. A weighed

**Table II Results of Mechanical Tests: Total Energy Absorbed During Impact ( $U_t$ ) at a Temperature of –10°C and Time  $F_{50}$  of Bent Strip Test for Copolymers**

Reference	$U_t$ (J)	$F_{50}$ (h)
Sample A	0.358	>2000
Sample B	0.600	>2000
Sample C	0.381	426.0
Sample D	0.419	296.2
Sample E	0.354	21.6

( $\cong 10$  mg) sample was first melted at 220°C for 10 min and then cooled at a rate of 20°C/min to 130°C, the highest temperature to be crystallized isothermally (60 min). Subsequently, the sample was subjected to a series of isothermal crystallization steps (duration 60 min) at intervals of 5°C, down to 60°C. The sample was then cooled to a temperature of 30°C, always at 20°C/min. Finally, a usual scanning reheating experiment from –20°C to 220°C at 5°C/min was then performed to reveal multiple melting peaks.

## RESULTS AND DISCUSSION

### Mechanical Properties

The total energy absorbed ( $U_t$ ) by each of the copolymers A, B, C, D, and E at a temperature of –10°C during the Charpy impact test is listed in Table II. MDPE sample B presents the highest value of all samples investigated and sample E the lowest value.

The time  $F_{50}$ , evaluated with the Bent Strip Test for the five samples, is also reported in Table II. As expected, MDPE copolymers A and B have better resistance to SCG than HDPE copolymers. Neither of the MDPE specimens failed in the ESCR test (interrupted after 2000 h) because they are too compliant. On the other hand, the Bent Strip Test clearly distinguished the three HDPE samples, even though their density values were very close to each other (0.944 g/cm<sup>3</sup>).

The total energy absorbed during impact on the Charpy specimens at –10°C can discriminate them, with sample B exhibiting the highest impact energy. The failure modes were of the semi-ductile type (postyield energy important and no drop in force after yield point with a gradual decrease of the registered force on a force-displacement–time diagram). A standard deviation

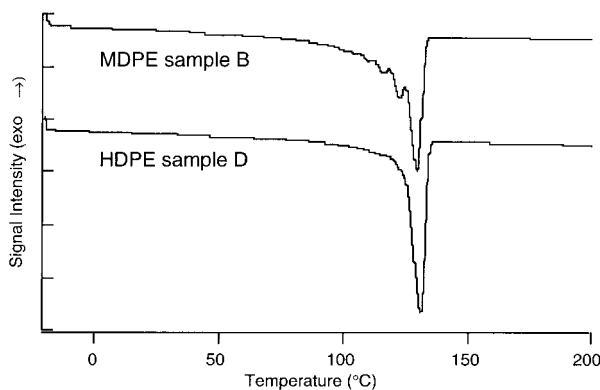


**Figure 2** SIST thermograms for samples B (MDPE) and D (HDPE).

of 5–10% of the average value is expected for the total impact energy.

### Fractionated PE Characterization

The stepwise isothermal segregation technique is a fractionation technique based, like TREF, on the crystallizability of the polymer chains, but operating in the melt.<sup>33</sup> The insertion of 1-hexene (as comonomer) along the macromolecular chains reduces the average sequence length of crystallizable ethylene units and consequently decreases the lamellar thickness. According to the Thomson–Gibbs relation,<sup>34</sup> as the amount of comonomers increases the more the melting point of the

copolymer is depressed with respect to the unsubstituted polymer.

Two SIST endotherms, representative of peculiar MDPE and HDPE behaviors, are shown in Figure 2. Variation of the cumulated enthalpy with temperature is traced in Figure 3. HDPE samples have a higher peak melting point than that of MDPE samples (with concomitant thicker lamellae) and a somewhat narrower distribution of lamellar thicknesses. Differences, in terms of crystallizability, among samples characterized in this study were confirmed by SIST.

The PTREF profiles, showing weight fraction distribution with elution temperature, are plotted in Figures 4(a) and (b). MDPE samples are characterized by a bimodal weight distribution. For HDPE copolymers, the distribution is not bimodal, but either unimodal (samples C and E) or trimodal (sample D). The evolution of the cumulated weight fractions with elution temperature is traced in Figure 5. Examination of Figures 4 and 5 confirms the density classification established by pycnometry. For the MDPE group, more matter is collected at lower elution temperatures (40, 50, 60, 70, and 80°C).

SCB content and molar mass data obtained when characterizing PTREF fractions, respectively, with NMR and SEC techniques, are summarized in Table III. The SCB content decreases with an increase of elution temperature. Such branches reduce the average ethylene sequence length and then restrict the formation of thick

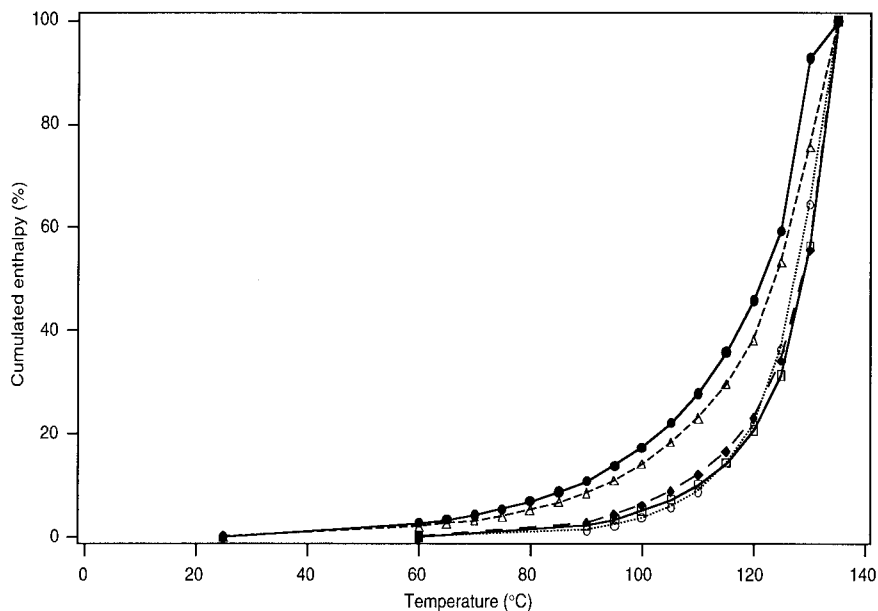


**Figure 3** SIST: cumulated enthalpy versus temperature for PE copolymers A ( $\Delta$ ), B ( $\bullet$ ), C ( $\circ$ ), D ( $\square$ ), and E ( $\blacklozenge$ ).

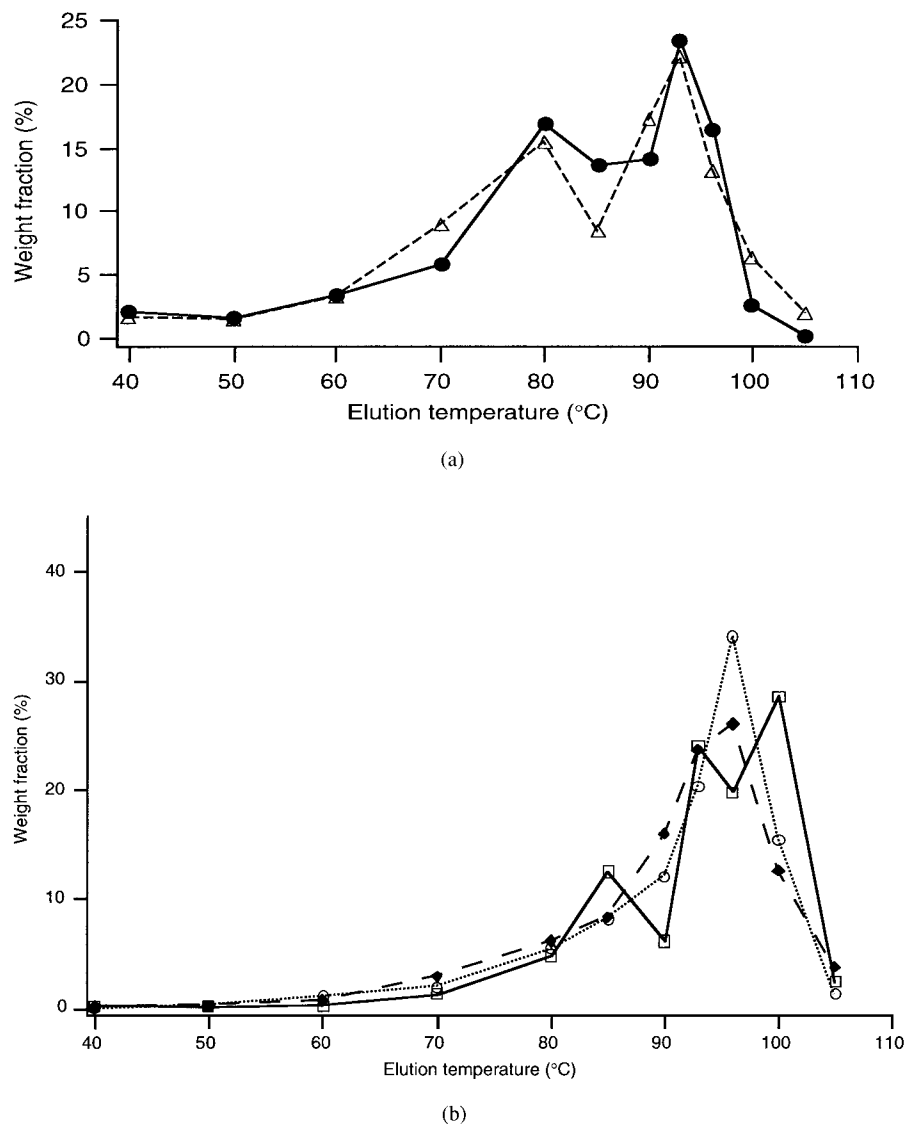


**Figure 4** PTREF diagrams: weight fractions versus elution temperature for MDPE samples (a) and HDPE samples (b).

lamellae, thus contributing to the reduction of polymer crystallinity. Typical SEC chromatograms of fractions corresponding to increasing elution temperatures are presented in Figure 6. Figure 6(a) and (b) are observed at elution temperatures lower than 90°C, and Figure 6(c) at 90°C or more. At low elution temperatures, two distinguishable SEC peaks (called  $M_{p1}$  and  $M_{p2}$ ) are observed. The ratio of the concentrations of the short molecules peak ( $M_{p1}$ ) to the longer molecules peak ( $M_{p2}$ ) decreases with elution temperature up to 90°C. From this temperature, a single SEC peak ( $M_{p2}$ ) is observed.

It should be emphasized that these molar mass peak values decrease with a decrease of elution

temperature. Peak values, rather than classical average molar mass values, are used in this study, a choice that was made essentially because of the lack of physical sense of  $M_w$  values for bimodal distributions. More precisely, we define  $M_{pavg}$  mass (the average of  $M_{p1}$  and  $M_{p2}$  peak SEC values) to better describe the length of the molecules in the case of bimodal SEC distributions.

Two populations of molecules (one of short chains and one of long chains) can thus be confirmed, thus implying the existence of different types of active catalytic sites, already proposed in Ziegler–Natta catalysts by Usami<sup>35</sup> from the observation of PTREF diagrams.

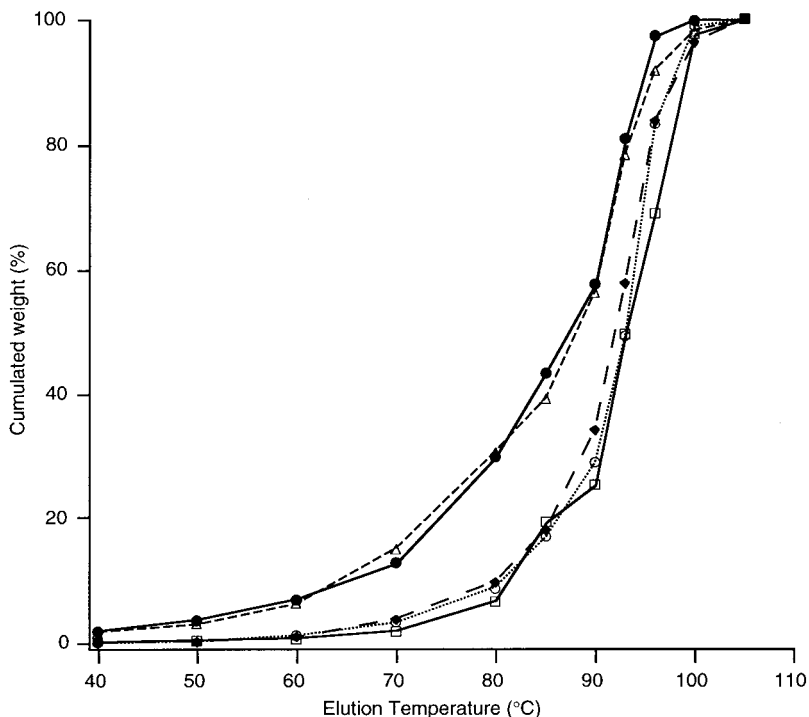


**Figure 5** Cumulated weight versus elution temperature for MDPE samples A ( $\Delta$ ) and B ( $\bullet$ ); and for HDPE samples C ( $\circ$ ), D ( $\square$ ), and E ( $\blacklozenge$ ).

The decrease of the SCB content with elution temperature can be interpreted as follows: the two types of active sites have different characters in the polymerization of ethylene with 1-hexene. One type produces short and branched molecules, whereas the other type yields fewer branched but longer molecules. The proportion of the molecules obtained with the second type of site increases with elution temperature.

The PTREF diagrams, described earlier, can then be interpreted. In bimodal distributions obtained for samples A and B, the peak appearing at low elution temperatures is representative of short and highly branched molecules, whereas longer and linear molecules are eluted at higher temperatures, giving rise to the second PTREF peak. On the contrary, for samples C and E of higher density, the distribution is not bimodal but unimodal. No significant matter is collected at lower elution temperatures. The peculiar trimodal diagram obtained with sample D must be seen as intermediate between the bimodal and unimodal diagrams. Indeed, this polymer contains more branched (see elution peak at 85°C) but also more linear molecules (see elution peak at 100°C) than those of samples C and E. Moreover, the fraction collected at 93°C includes molecules that are similar to those in MDPE samples but at the same

time much longer than molecules found in other HDPE samples.

The typical SCB distribution on macromolecules is plotted in Figure 7 for samples B (MDPE) and D (HDPE). In this figure, we can observe that intermolecular heterogeneity is nonoptimum in terms of SCGR for Cr-catalyzed PE copolymers: SCB content is higher on lower molar mass molecules. This situation was previously reported in the literature for Ziegler-Natta catalysts.<sup>24-27</sup> The pronounced decrease of SCB content with molar mass confirms the existence of the two types of molecules. In MDPE samples, SCB concentration is higher at given molar mass than for HDPE.

### Interpretation of Mechanical Results

Among the five copolymers analyzed in this study, differences in mechanical properties were confirmed by Bent Strip and Charpy tests. In the next part of this study, we explain such differences by exploiting results about molecular structure, presented earlier.

### Slow Crack Growth Resistance

It was previously reported that SCGR in PE pipes depends on the molecular structure of the PE



**Table III PTREF Fractions Characteristics**

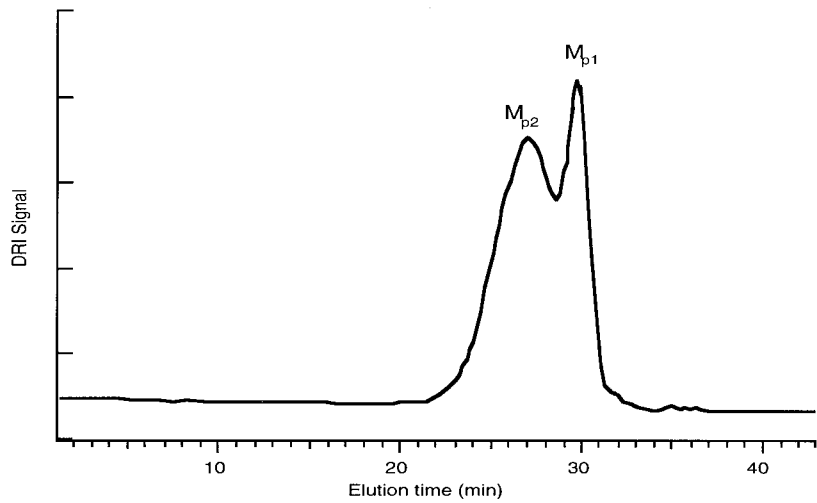
Reference	Elution Temperature (°C)	NMR: SCB <sup>a</sup>	SEC <sup>b</sup>	
			$M_{p1}$ <sup>b</sup> (daltons)	$M_{p2}$ <sup>b</sup> (daltons)
Sample A	40	313.7	700	18,100
	50	251.5	1900	26,100
	60	203.7	2300	26,300
	70	164.3	3800	33,100
	80	117.8	5600	36,900
	85	108.2	15,100	55,400
	90	70.5		26,600
	93	60.0		88,400
	96	44.2		87,400
	100	108.2		84,500
Sample B	105	39.8		89,400
	40	306.6	700	10,800
	50	242.4	2100	23,300
	60	204.5	2500	26,600
	70	155.1	3700	29,700
	80	112.1	8700	34,400
	85	77.7	17,800	46,500
	90	56.3		34,000
	93	38.2		72,800
	96	37.6		79,600
Sample C	100	30.7		89,000
	105	— <sup>c</sup>		— <sup>c</sup>
	40	— <sup>c</sup>	— <sup>c</sup>	— <sup>c</sup>
	50	— <sup>c</sup>	— <sup>c</sup>	— <sup>c</sup>
	60	— <sup>d</sup>	2200	18,900
	70	— <sup>d</sup>	2800	27,200
	80	99.9	4700	30,700
	85	73.3	7700	31,000
	90	51.1		15,400
	93	30.7		34,400
Sample D	96	26.1		85,500
	100	26.5		79,100
	105	35.9		54,800
	40	— <sup>c</sup>	— <sup>c</sup>	— <sup>c</sup>
	50	— <sup>c</sup>	— <sup>c</sup>	— <sup>c</sup>
	60	— <sup>c</sup>	— <sup>c</sup>	— <sup>c</sup>
	70	145.7	2900	27,400
	80	92	5000	33,800
	85	74.8	9100	27,500
	90	38.5		20,500
Sample E	93	36.7		80,900
	96	30.4		82,100
	100	22.6		83,600
	105	23.9		88,400
	40	— <sup>c</sup>	— <sup>c</sup>	— <sup>c</sup>
	50	— <sup>c</sup>	— <sup>c</sup>	— <sup>c</sup>
	60	— <sup>d</sup>	2200	10,500
	70	131.0	3200	24,700
	80	87.5	5300	29,000
	85	78.4	9500	29,000
	90	46.0		18,500
	93	47.4		34,600
	96	27.4		76,500
	100	33.7		83,600
	105	37.9		86,500

<sup>a</sup> Methyl content obtained with <sup>1</sup>H-NMR (/10,000 C).

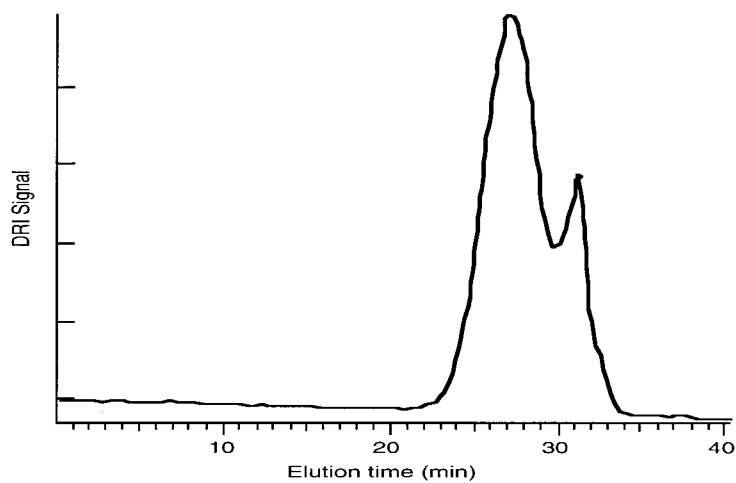
<sup>b</sup>  $M_{p1}$  is the molar mass of the SEC peak corresponding to the lowest molar masses distribution for PTREF fractions. The other is denoted  $M_{p2}$ . From an elution temperature of 90°C, only one SEC peak is considered (see Fig. 6). This peak is also noted  $M_{p2}$ .

<sup>c</sup> PTREF matter collected inferior to 0.5% of the total weight.

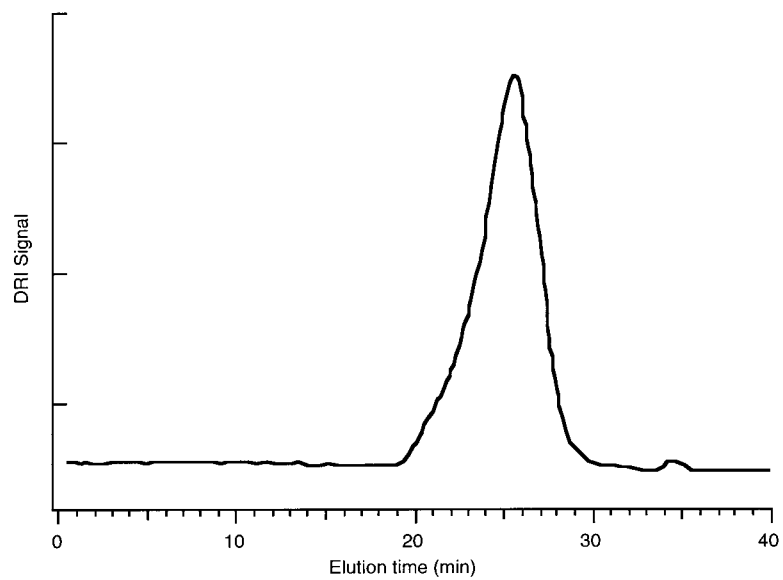
<sup>d</sup> No possibility of NMR characterization.



(a)



(b)



(c)

**Figure 6** Typical SEC chromatograms of PTREF fractions observed at increasing elution temperatures: (a and b) temperatures lower than 90°C; (c) temperatures above 90°C.

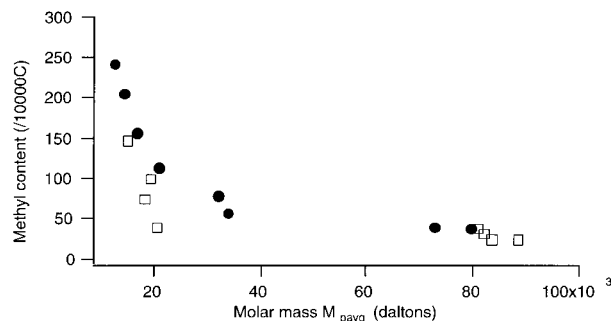


**Figure 7** Methyl content versus molar mass  $M_{p2}$  ( $M_{pavg}$  for bimodal SEC distributions of PTREF fractions eluted at lower temperatures) for MDPE sample B (●) and HDPE sample D (□).

chains,<sup>3–15</sup> especially on their molar mass and SCB content. SCGR is increased with longer and more branched chains.

From our results, it appears that SCGR mainly depends on SCB content. As observed before in Table II, time  $F_{50}$ , representative of SCGR, is above 2000 h for MDPE and is under 500 h for all HDPE samples. To explain this, it can be observed that, as expected, MDPE samples are characterized by a greater butyl content, measured by  $^{13}\text{C}$ -NMR and reported in Table I: SCB content in MDPE is nearly three times greater than that of HDPE. The presence of very branched molecules in MDPE samples has been confirmed by SIST and TREF fractionation techniques.

HDPE samples present contrasted SCGR where 426.0, 296.2, and 21.6 are the time  $F_{50}$  values (in h) for samples C, D, and E, respectively. These differences cannot be explained by differences in SCB content. The three samples possess similar density and butyl content. Low SCGR of sample E can be explained by examination of average  $z$ -average molar mass ( $M_z$ ) values in Table I. Indeed, whereas samples C and D present similar  $M_z$  values, sample E is characterized by a much lower value.

Differences in molecular structures of samples C and D have to be confirmed to explain their contrasted  $F_{50}$  values: time  $F_{50}$  of sample C is almost twice that of sample D (Table II). These differences have been highlighted by PTREF technique, in combination with SEC and NMR characterization techniques. A new index, the “SCG index,” is proposed in this study: it is defined as the maximum value of the product, for each PTREF fraction, of methyl content, molar mass  $M_{p2}$  ( $M_{pavg}$  for bimodal SEC distributions observed at lower elution temperatures), and

PTREF fraction weight. This index takes into account the fact that SCGR depends on SCB content and on length of macromolecules but also on the distribution of SCB on the different macromolecules (intermolecular heterogeneity). The calculated values of this index are reported in Table IV for HDPE samples. For each sample, the maximum index value is representative of the most efficient molecules, in terms of SCGR. The best SCGR of sample C is correlated with the highest maximum index value of all HDPE samples, whereas the lowest SCGR of sample E, already explained in terms of lowest  $M_z$  value, is confirmed by the lowest maximum SCG index. HDPE sample C possesses, in sufficient quantity (34% of total sample weight), relatively branched mole-

**Table IV** “SCG Index” Values for HDPE Copolymers

Reference	Elution Temperature (°C)	“SCG Index” <sup>a</sup>
Sample C	40	—
	50	—
	60	—
	70	—
	80	97,200
	85	116,000
	90	95,200
	93	213,300
	96	758,700
	100	322,800
	105	25,600
Sample D	40	—
	50	—
	60	—
	70	28,600
	80	85,700
	85	171,100
	90	48,100
	93	717,600
	96	508,100
	100	526,300
	105	50,700
Sample E	40	—
	50	—
	60	—
	70	51,000
	80	91,300
	85	124,900
	90	135,300
	93	387,000
	96	545,000
	100	355,000
	105	121,300

<sup>a</sup> Maxima “SCG index” values are italicized.

**Table V** “Mass Index” Values for PE Polymers

Reference	“Mass Index”
Sample A	51,500
Sample B	46,900
Sample C	53,700
Sample D	66,200
Sample E	47,800

cules that are long enough to entangle efficiently (methyl content of 26/10,000 C and  $M_{p2}$  of 85,000 daltons).

### Rapid Crack Propagation Resistance

It was previously reported that impact fracture toughness mainly depends on the length of macromolecules.<sup>19–21</sup> Thus RCPR is improved with longer chains. The influence of density on RCPR is not very well defined. Fleissner<sup>19</sup> reported a density value of 0.934 (at room temperature), above which impact fracture toughness is nearly independent of density.

SCB content influence on RCPR seems very clear for sample B, which is the most branched, with a butyl content of 68/10,000 C (Table I). Indeed, this MDPE, characterized by the lowest density value (0.933), possesses the highest total absorbed impact energy (Table II). This influence disappears, however, for MDPE sample A (density of 0.937 and butyl content of 54/10,000 C, Table I). Indeed, this sample is characterized by an energy  $U_t$  lower than that of HDPE samples C and D. It can thus be concluded that, as indicated by Fleissner,<sup>19</sup> above a density located around 0.934, impact fracture toughness is independent of density. Thus impact energy variations for products with a density above 0.937 (i.e., samples A, C, D, and E) must be explained by the length differences of macromolecules. It is hazardous to emphasize such differences by observing single  $M_w$  or  $M_z$  values obtained with the SEC technique. The very wide molar mass distribution of these multisite catalyzed PEs must also be taken into account.

A new method is proposed in this study, thanks to PTREF–SEC results: the use of a rather new index, called “mass index,” which is defined for each sample as the sum, on all PTREF fractions, of the product of molar mass  $M_{p2}$  ( $M_{pavg}$  for bimodal SEC distributions) and weight fraction PTREF. Use of peak values for PTREF fractions makes more sense because of the narrow molar

mass distribution of these fractions. The calculated values are reported in Table V. The variation of total impact energy, measured at the temperature of  $-10^\circ\text{C}$ , with “mass index” value is plotted in Figure 8. It can be observed that, for samples A, C, D, and E, RCPR results correlate relatively well with the mass index values. Indeed, RCPR increases when the mass index becomes greater. It must be noticed that MDPE sample B, which presents the best RCPR, is also characterized by the lowest mass index value. It confirms that this favorable mechanical behavior is mainly attributed to the presence of numerous branchings.

### CONCLUSIONS

Correlations have been attempted between parameters describing molecular structure and mechanical properties. It has been shown that characterization of molecular structure of neat polymers by conventional analytical techniques (NMR, SEC, DSC) is not sufficient to establish such relationships. However, PTREF fractionation, with respect to crystallizability, followed by DSC, NMR, and SEC techniques, provides a very effective tool to elucidate molecular structure of PE copolymers. PTREF histograms obtained were different for each of the five copolymers studied, relating each repartition of crystallizable ethylene sequences. It was also shown that intermolecular heterogeneity of Cr-catalyzed PE copolymers is not optimum in terms of SCGR: SCBs are mainly located on shorter molecules. However, the main drawback of PTREF is the cumbersome procedure to be followed, and its time-consuming aspect. In this respect, it is important that SIST results be used to predict TREF results, as we

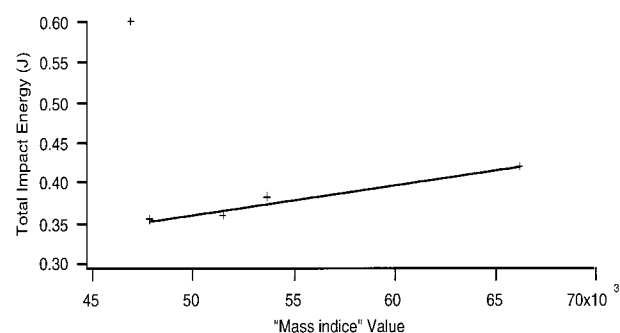


**Figure 8** Total impact energy (measured at  $-10^\circ\text{C}$ ) versus “mass index” value.

have shown. SIST thermograms may then be used to construct TREF temperature profiles.

To explain the obtained mechanical results, two new indices have been proposed: the "SCB index" and the "mass index." It appears that SCGR depends mainly on SCB content, whereas impact fracture toughness is mainly related to the length of the molecules. Indeed, it has been observed that energy absorbed during the impact test is independent of density when the density value is above 0.937. This result confirms previous observations made by Fleissner.<sup>19</sup>

The analysis presented here certainly suggests two areas that may be worthy of further study. The first concerns the interest of fractionation with respect to molar mass, and not to crystallizability. The second concerns an improved definition of the new indices proposed in this study.

The authors gratefully acknowledge G. Lobet and L. Verhofstede for their assistance, J. Defour and staff for their help with mechanical tests, M. Lamotte for NMR measurements (Fina Research), A. Jonas for valuable remarks, M. Deparadis for training in PTREF technique, and B. van der Heyden for help with DSC experiments (Unité de Physique et de Chimie des Hauts Polymères). The authors acknowledge La Région Wallonne for the financial support.

## REFERENCES

- Scheirs, J.; Böhm, L. L.; Boot, J. C.; Leever, P. S. *TRIP* 1996, 4, 408.
- Usclat, D. Personal communication.
- Huang, Y. L.; Brown, N. *J Polym Sci Polym Phys Ed* 1991, 29, 129.
- Lu, X.; McGhie, A. R.; Brown, N. *J Polym Sci, Polym. Phys. Edn.* 1992, 30, 1217.
- Huang, Y. L.; Brown, N. *J Polym Sci Polym Phys Ed* 1990, 28, 2007.
- Lu, X.; Ishikawa, N.; Brown, N. *J Polym Sci Polym Phys Ed* 1996, 34, 1802.
- Lustiger, A.; Markham, R. L. *Polymer* 1983, 24, 1647.
- Brown, N.; Lu, X.; Huang, Y. L. *Makromol Chem Macromol Symp* 1991, 41, 55.
- Lu, X.; Brown, N. *J Mater Sci* 1986, 21, 2433.
- Lustiger, A.; Markham, R. L. in *Optimizing the Resistance of Polyethylene to Slow Crack Growth*, Proceedings of Plastic Pipes VI, The Plastic and Rubber Institute, York, 1985.
- Böhm, L. L.; Enderle, H. F.; Fleissner, M. *Adv Mater* 1992, 4, 231.
- Lu, X.; Wang, Q.; Brown, N. *J Mater Sci* 1988, 23, 643.
- Bubeck, R. A.; Baker, H. M. *Polymer* 1982, 23, 1680.
- Ishikawa, N.; Shimizu, T.; Shimamura, Y.; Goto, Y.; Omori, K.; Misaka, N. Presented at Proceedings of the Tenth Plastic Foul Gas Pipe Symposium, American Gas Association, 1987.
- Scholten, F. L.; Rijpkema, H. J. M. Presented at Proceedings of Plastic Pipes VIII, The Plastic and Rubber Institute, London, 1992.
- Qian, R.; Brown, N. *Polymer* 1993, 34, 4727.
- Qian, R.; Lu, X.; Brown, N. *Polymer* 1993, 34, 4727.
- Van Speybroeck, P.; Van Speybroeck, H. Utilisation de polyéthylènes pour des réserves gaz sous 10 bars. Rêve ou réalité, Rapport de l'Association technique de l'industrie du gaz, 1996.
- Fleissner, M. *Angew Makromol Chem* 1982, 105, 167.
- Deanin, R. D. *Polymer Structure, Properties and Applications*; Cahners: Boston, 1972.
- Dayal, U.; Mathur, A. B.; Shashikant *J Appl Polym Sci* 1996, 59, 1223.
- Channell, A. D.; Clutton, E. Q. *Polymer* 1992, 33, 4108.
- Lu, X.; Qian, R.; Brown, N. *Polymer* 1995, 36, 4239.
- Spitz, R.; Saudemont, T. *Chim Nouvelle* 1996, 14, 1643.
- Böhm, L. L. *Makromol Chem* 1981, 182, 3291.
- Defoor, F.; Groeninckx, G. *Polymer* 1992, 33, 3878.
- Scholten, F. L.; Zefrin, R. B.; Smeltink, M. G. in *Evaluation of European (GERG) PE materials*, IEA International Conference on Natural Gas Technology, Berlin, 1996.
- Leever, P. S.; Vayla, P.; Wheel, M. A. *Plast Rubber Compos Process Appl* 1992, 17, 247.
- Marshall, G. P.; Ingham, E. J. in *The Contribution of Plane Stress and Plane Strain Components into the Fast Fracture Resistance of Polyethylene Pipe Materials, Deformation, Yield and Fracture of Polymers*, Proceedings of PRI 10th International Conference, 1997; p. 110.
- Wild, L.; Ryle, T. *Polym Prepr (Am Chem Soc Div Polym Chem)* 1977, 18, 182.
- Scheinert, W. *Angew Makromol Chem* 1977, 63, 117.
- Otocka, E. P.; Roe, R. J.; Helamn, N. Y.; Muglia, P. M. *Macromolecules* 1971, 4, 507.
- Kamiya, T.; Ishikawa, N.; Kambe, S.; Ikegami, N.; Nishibu, N.; Hattoki, T. *SPE ANTEC '90*, 871.
- James, D. E. *Encycl Polym Sci Eng* 1986, 6, 429.
- Usami, T.; Gotoh, Y.; Takayama, S. *Macromolecules* 1986, 19, 2722.